Novel fluorescence molecular imaging of chemotherapy-induced intestinal apoptosis

Galit Levin*
Anat Shirvan*
Hagit Grimberg
Ayelet Reshef
Merav Yogev-Falach
Avi Cohen
Aposense Ltd.
5 Ha'Odem Street
P.O. Box 7119
Petach-Tiqva 49170
Israel

Ilan Ziv
Aposense Ltd.
5 Ha'Odem Street
P.O. Box 7119
Petach-Tiqva 49170
and
Tel-Aviv University
Sackler School of Medicine
Tel-Aviv
and
Rabin Medical Center
Department of Neurology
Petach-Tiqva 49100
Israel

Abstract. Chemotherapy-induced enteropathy (CIE) is one of the most serious complications of anticancer therapy, and tools for its early detection and monitoring are highly needed. We report on a novel fluorescence method for detection of CIE, based on molecular imaging of the related apoptotic process. The method comprises systemic intravenous administration of the *ApoSense* fluorescent biomarker (N,N′-didansyl-L-cystine DDC) *in vivo* and subsequent fluorescence imaging of the intestinal mucosa. In the reported proof-of-concept studies, mice were treated with either taxol +cyclophosphamide or doxil. DDC was administered *in vivo* at various time points after drug administration, and tracer uptake by ileum tissue was subsequently evaluated by *ex vivo* fluorescent microscopy. Chemotherapy caused marked and selective uptake of DDC in ileal epithelial cells, in correlation with other hallmarks of apoptosis (i.e., DNA fragmentation and Annexin-V binding). Induction of DDC uptake occurred early after chemotherapy, and its temporal profile was parallel to that of the apoptotic process, as assessed histologically. DDC may therefore serve as a useful tool for detection of CIE. Future potential integration of this method with fluorescent endoscopic techniques, or development of radio-labeled derivatives of DDC for emission tomography, may advance early diagnosis and monitoring of this severe adverse effect of chemotherapy. [DOI: 10.1117/1.3253303]

Keywords: molecular imaging; apoptosis; cell death; chemotherapy; ApoSense; gastrointestinal damage; optical imaging.

Paper 09204R received May 20, 2009; revised manuscript received Aug. 1, 2009; accepted for publication Aug. 4, 2009; published online Oct. 27, 2009; corrected Oct. 7, 2011.

1 Introduction

Chemotherapy-induced enteropathy (CIE), i.e., damage to the intestinal mucosa, induced by anticancer drugs, is one of the most prevalent and serious adverse effects of anticancer treatments. Related symptoms range from nausea, vomiting, abdominal pain, and diarrhea to gastrointestinal bleeding, perforation, and sepsis. The severity of CIE is often unpredictable, and it manifests large interpatient variability. Furthermore, its concurrence with drug-induced myelosuppression may be life threatening.[1–4] In addition, CIE is often a major limiting factor in effective tumor control because it often leads to undesirable reduction in drug dosage or prolongation of the interdose interval, thus hampering effective tumor control. Early detection of CIE may therefore assist in taking preventive measures, deciding on specific treatments to inhibit progression of this damage, or selecting an alternative protocol of anticancer therapy. Currently, diagnosis of CIE is made only on translation of the intestinal damage into overt clinical symptoms and signs. Conceivably, a diagnostic tool, capable of early and sensitive detection of CIE *in situ*, at its occurrence at the tissue level rather than at the level of its unpleasant, painful, and potentially life-risking consequences, may be highly beneficial for treatment optimization for the individual cancer patient.

Numerous lines of evidence indicate that death of the epithelial cells lining the intestinal mucosa is the major histopathological substrate of CIE.[1,2,5] Specifically, apoptosis has been shown to play an important role in this toxic effect of chemotherapy, triggered in response to drug-related damage to DNA, proteins and/or cellular metabolic pathways.[1,6–9]. We therefore hypothesized that molecular imaging of apoptosis may serve as a useful tool for early detection of CIE. (*N*,*N*′-didansyl-L-cystine DDC) is a member of the *ApoSense* family of low-molecular-weight compounds, designed for imaging of apoptosis *in vivo*.[10–15] This novel class of molecular probes responds to a complex of cellular features, unique to cells in early apoptosis, comprising irreversible loss of transmembrane potential, permanent acidification of the outer plasma membrane and cytosol, and activation of membrane phospholipid scramblase, all occurring from the early stages of the death process, while membrane integrity is still pre-

*These authors contributed equally to the work.
Address all correspondence to: Marav Yogev-Falach, PhD, Aposense Ltd., 5 Ha'Odem Street, P.O. Box 7119, Petah-Tiqva 49170, Israel. Tel: 972-3-9215717 or 972-3-9247211; Fax: 972-3-9227581; E-mail: merav@aposense.com

1083-3668/2009/14(5)/054019/8/$25.00 © 2009 SPIE

served. Respectively, DDC performs selective binding and uptake through the cell membrane of the apoptotic cell, and accumulates within the cytoplasm.[10–15] Previously, DDC has been shown to be useful in detection of apoptosis in various preclinical models of disease, such as acute renal failure, experimental cerebral stroke and traumatic brain injury.[10,11,13,14] In addition, in models of cancer, increased DDC uptake was observed on induction of tumor cell death by chemotherapy. This increased DDC uptake was detectable before alterations in tumor size and was found to correlate with subsequent increased animal survival.[11]

This profile of DDC prompted us to explore its potential utility also for *in situ* detection of CIE. Because DDC is capable, on its systemic administration *in vivo*, to selectively reach and bind to cells undergoing apoptosis, as demonstrated in numerous models investigated to date, we hypothesized that this approach can also be applied to the detection of intestinal damage induced by chemotherapy. This hypothesis was therefore examined in the current study. The experimental paradigm comprised systemic administration of chemotherapy to tumor-bearing mice, thus inducing apoptosis, followed by intravenous administration of DDC *in vivo*. Ileum and tumor tissues were then subsequently subjected to *ex vivo* fluorescent microscopy, for detection of DDC-positive apoptotic cells. The temporal profile of uptake of the probe, as well as its correlation with other markers of apoptosis was also characterized.

2 Material and Methods

2.1 *Materials*

DDC[10,13] was synthesized as previously described. Compound was dissolved in 0.1 M phosphate buffer (pH 7.4). Apoptag® Fluorescein Direct Kit (TUNEL, S7160) was purchased from Intergen Inc. New York. Annexin-V-Cy3 (Apoptosis Detection Kit) was obtained from BioVision Inc., Palo Alto, California. Taxol (Paclitaxel) was supplied by Bristol-Myres Squibb, Syracuse, New York. Cyclophosphamide, hematoxylin, and eosin were obtained from Sigma, St. Louis, Missouri. Doxil [doxorubicin HCl liposome injection (Ben Venue Laboratories, Inc., Bedford, Ohio)] was supplied as a ready-to-use sterile solution of 2 mg/mL.

2.2 *Animals and Induction of Tumor Model*

Male Balb/C mice [8–10 weeks old, 20–25 g (Harlan Inc., Jerusalem, Israel)] were used for this study. All animal studies were performed according to the Guiding Principles for Research Involving Animals, and study protocols were approved by the local Animal Care Committee. Murine colon adenocarcinoma cells (CT-26, CRL-2638) were obtained from ATCC, Rockville, Maryland, and were cultured in RPMI 1640 medium, containing 2 mM of L-glutamine, 100 units/mL of penicillin, 100 μg/mL of sterptomycin, and 10% heat inactivated FBS. Cell cultures were incubated in flasks at 37 °C in a humid 5% CO_2-95% air environment and seeded at a concentration of $1-2\times10^5$ cells/mL. Cells were trypsinized, washed twice with HBS (140 mM NaCl; 0.5 M Hepes, pH 7.4), and centrifuged (5 min, 1000 rpm, at room temperature), dispersed into single cells and concentrated into 13.3×10^6 cells/mL. Mice were injected subcutaneously, at the flank, each with a volume of 30 μL of this cell solution (4×10^5 cells/dose) under ketamine anesthesia [100 mg/kg, intraperitonal injection (i.p.)].

2.3 *Systemic Administration of Chemotherapy and DDC*

Animals at each group ($n=5$ per group) were subjected to a single administration of one of the following chemotherapeutic regimens: (*i*) A combination of taxol and cyclophosphamide (Tx+CPA), administered by the intraperitoneal route, at a dose of 20 mg/kg and 200 mg/kg, respectively, and (*ii*) doxil, administered intravenously at a dose of 20 mg/kg. Untreated animals served as controls. At 24 h after chemotherapy, or at various time points of the temporal profile study, animals were injected intravenously with DDC (1.4 mg/mouse) and Annexin-V-Cy3 in aqueous buffered solution (0.22 mL/mouse, according to manufacturer's instructions). Two hours later, mice were sacrificed by cervical dislocation; tissues of the ileum and tumors were excised and frozen immediately. Ten-micron cryosections were then prepared (Cryostat, Leica, DM) and used for florescent microscopy. The time point of 2 h was chosen based on a preparatory calibration experiment, which quantified signal/background at the small intestine tissue at 0.5, 2, 4, and 6 h after DDC administration, utilizing the Spectral View® spectral imaging system (Applied Spectral Imaging, Migdal HaEmek, Israel). The study indicated that all three latter time points, (i.e., 2, 4, and 6 h after administration) were suitable for assessment, with persistence of the signal in the apoptotic cells.

2.4 *Histological Evaluation of DDC Uptake*

Cellular uptake of DDC and Annexin-V-Cy3 following intravenous administration *in vivo* was visualized and photographed in consecutive slides *ex vivo*, using a fluorescence microscope (BX51, Olympus Optical Co., London) equipped with a UMNU2 filter to detect the inherent fluorescence of DDC (excitation at 360–370 nm, emission at 420 nm), and a UMNG2 filter to detect the fluorescence of Annexin-V-Cy3 (excitation at 530–550 nm and emission at 590 nm). Signal/background (S/B) ratios of DDC versus Annexin-V were assessed by measurement of the intensity of the fluorescent signal in 40 random fields, utilizing the Spectral View spectral imaging system. Consecutive slides were also subjected to the terminal deoxynucleotidyl transferase biotin-dUTP nick end labeling (TUNEL) assay,[16] for detection of the characteristic apoptotic DNA fragmentation. The TUNEL assay was used according to manufacturer's instructions and visualized utilizing a UMNIBA2 filter (excitation at 470–490 nm, emission at 510 nm). In addition, consecutive slides were also subjected to standard hematoxylin and eosin (H&E) histological staining. Detection of apoptotic cells in the H&E staining was performed based on their characteristic morphology, comprising cell shrinkage, condensed and fragmented nuclei, and eosinophilic cytoplasm.[17]

2.5 *Assessment of Time-Course of the Chemotherapy-Induced Apoptosis*

For time-course experiments, animals were injected intravenously *in vivo* with DDC as described above, at different time

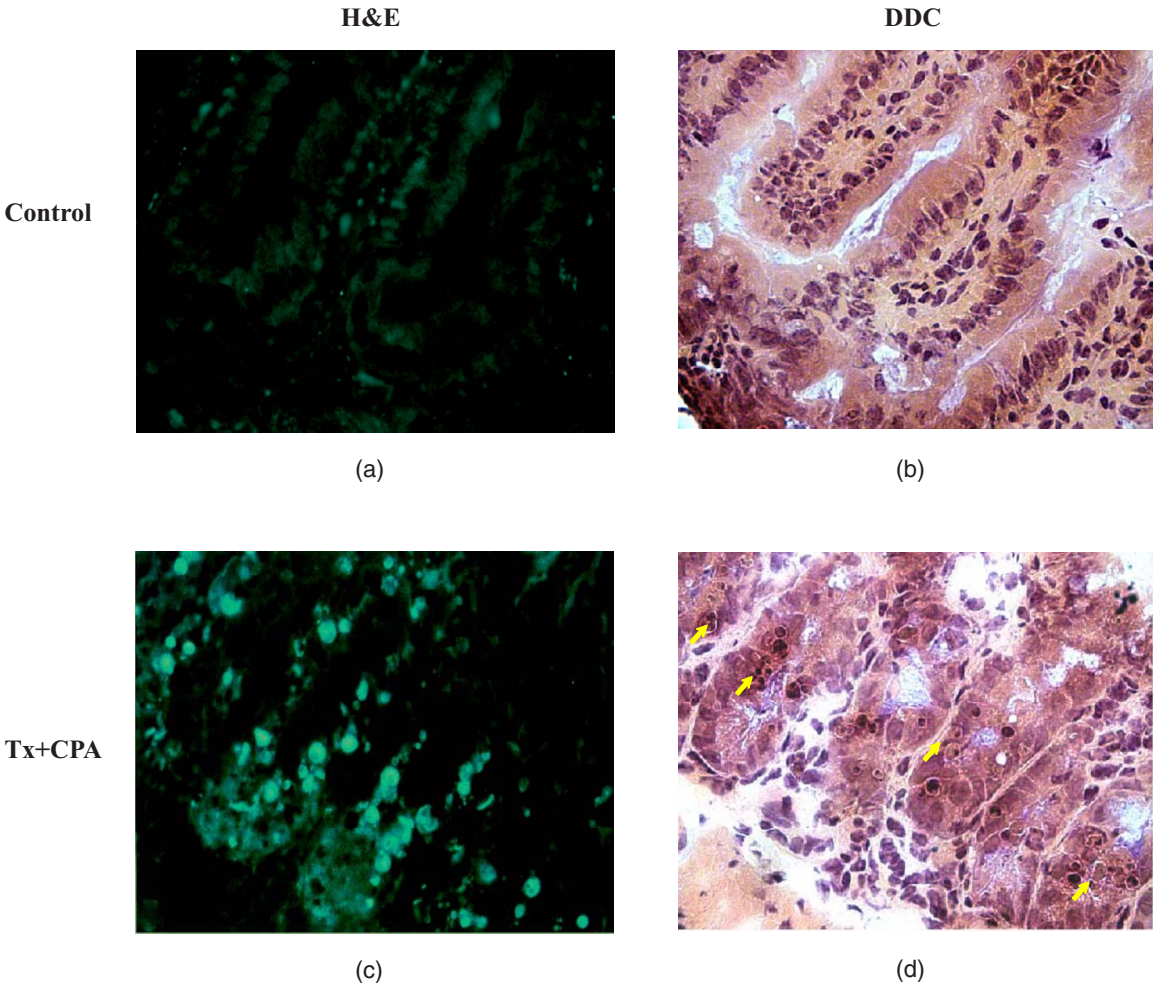

Fig. 1 Induction of apoptosis and emergence of DDC-positive cells in the small intestine epithelium in response to chemotherapy. Mice were treated with a single dose of taxol and cyclophosphamide (Tx+CPA, 20 mg/kg and 200 mg/kg, respectively, i.p.); 24 hours later, animals were injected with DDC (1.4 mg/mouse, intravenous) and sacrificed 2 h later. Small intestine tissue was then subjected to fluorescent microscopy, and standard H&E staining was performed on consecutive slides. Untreated mice served as controls. (a) Fluorescent microscopy of tissue from a control animal: only a few cells manifest DDC uptake; (b) respective H&E staining of control tissue; (c) fluorescent microscopy of tissue from a chemotherapy-treated mouse, revealing numerous cells that manifest DDC uptake; (d) respective H&E staining of the tissue from the chemotherapy-treated animal; numerous cells manifesting apoptotic morphology: cell detachment, nuclear condensation and fragmentation, and eosinophilic cytoplasm (some of these cells are indicated by the arrows).

points during a 70-h period after administration of Tx +CPA, or during a 160-h period after administration of doxil. Two hours later, animals were sacrificed, and tissues of the ileum and tumor were subjected to the *ex vivo* tissue processing described above. For each animal, consecutive slides of ileal tissue were subjected to two parallel analyses, performed by independent observers, each counting apoptotic cells in the crypts of the mucosa, wherein the apoptotic cells have been independently identified by either DDC uptake assessed by fluorescent microscopy, or histological assessment with H&E. Group analysis was then performed for each time point, comparing the mean number of apoptotic cells targeted by DDC (*in vivo* administration) to the number of apoptotic cells determined by the standard H&E histological assessment. Significance of intergroup differences was assessed by t-test, with a significance threshold of $p < 0.05$. In order to compare the time course of chemotherapy-induced apoptosis in the ileum, as detected by DDC, to that taking place at the tumor, tumor tissue was also obtained at the various time points after doxil administration, and subjected to fluorescent microscopy. For each slide of tumor tissue, the number of apoptotic cells per square millimeter was determined, utilizing the Spectral View spectral imaging system.

3 Results

Only few apoptotic cells were observed in the epithelium of the ileum obtained from control untreated animals, as assessed by standard H&E [Fig. 1(b)] staining. Respectively, only a small number of DDC-positive cells were observed [Fig. 1(a), magnification 400×]. By contrast, a single dose of chemotherapy caused the emergence of numerous cells that manifested DDC uptake [Figs. 1(c) and 2(a)], as assessed histologically 24 h later. Each of these cells manifested intracellular accumulation of the tracer, thus creating a high S/B ratio [Fig. 1(c) versus 1(a)]. This emergence of DDC-positive cells

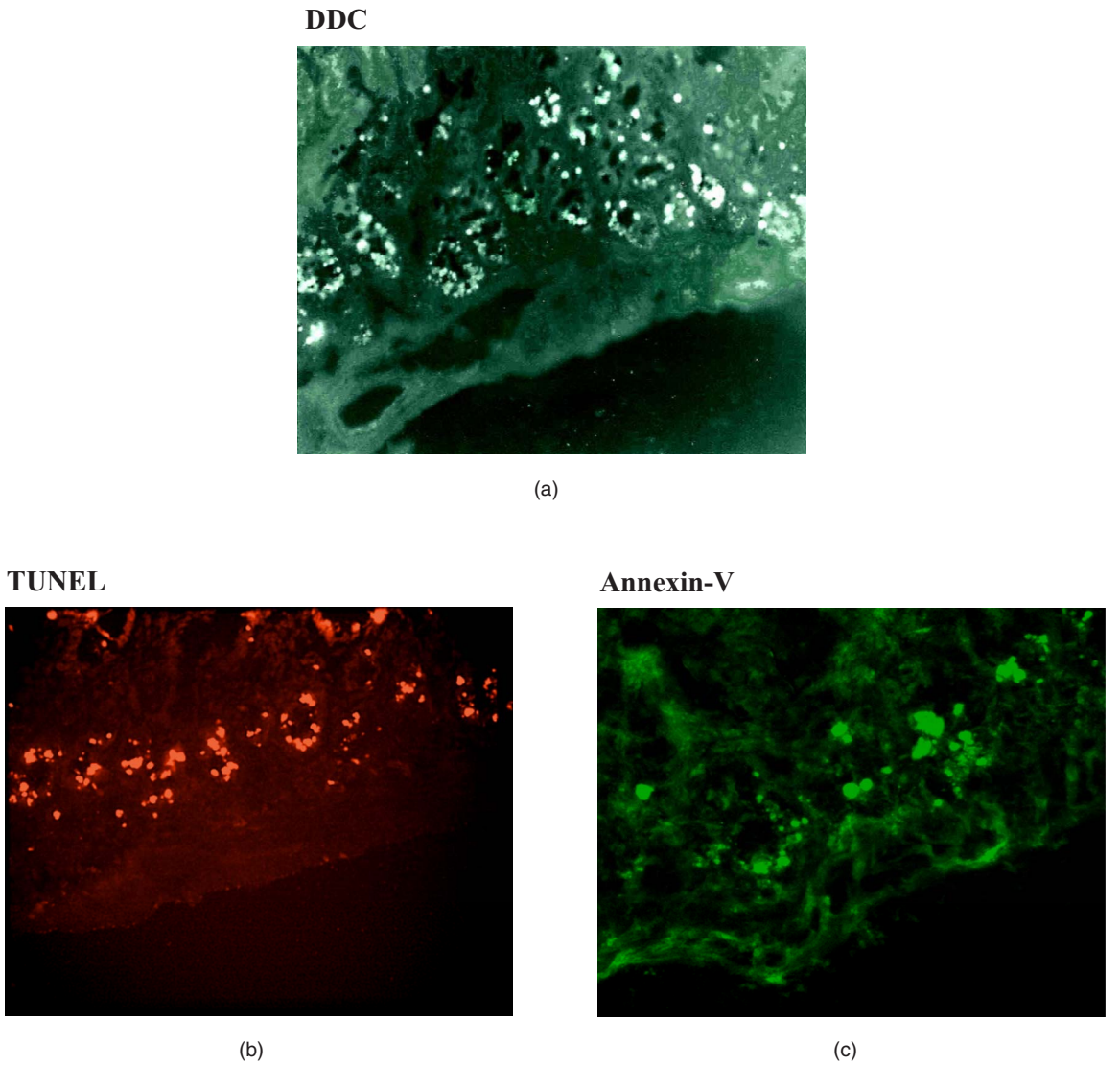

Fig. 2 DDC uptake versus TUNEL staining and Annexin-V binding in response to chemotherapy in small intestine epithelium in mice. Mice were treated with a single dose of Tx+CPA as described above, and at 24 h, administrated intravenously with either DDC or Annexin-V-Cy3. Two hours later, animals were sacrificed, and the small intestine (ileal) tissue was excised and subjected to cryosections. DDC or Annexin-V-Cy3 fluorescence was detected by the respective filters, as described in Sec. 2. Consecutive slides were also subjected to TUNEL staining, for detection of apoptotic DNA fragmentation. (a) DDC-uptake: a characteristic pattern of uptake in a chemotherapy-treated animal, with numerous cells in the intestinal crypts, manifesting uptake and intracellular accumulation of DDC, resulting in a strong signal; (b) respective TUNEL staining; and (c) respective Annexin-V-Cy3 uptake.

following chemotherapy was in alignment with detection of apoptotic cells by the H&E staining [Fig. 1(d)], and with the emergence of numerous TUNEL-positive cells in the intestinal crypts after chemotherapy (Fig. 2). As exemplified in Fig. 2, the extent of detection of apoptotic cells by intravenously administered DDC was high, similar to that of the TUNEL staining *in vitro*. Extent of detection by DDC was also markedly higher than that observed following of intravenously administered Annexin-V (Annexin-V-Cy3). This was reflected in both the number of detected cells and in the S/B ratios, measured as described above. The S/B ratio observed for DDC was 12.5 ± 1.9 (mean $\pm$ SD), versus a ratio of 3.5 ± 0.6, which was observed for Annexin-V ($p < 0.001$).

We then investigated the temporal profile of induction of DDC-positive cells by chemotherapy. For that purpose, apoptosis in the intestinal mucosa was independently evaluated in consecutive slides, by either DDC or standard H&E assessment,[18] at various time points after administration of a single dose of either taxol+cyclophosphamide or doxil. As shown in Fig. 3, administration of each of the chemotherapeutic regimens induced a marked and well-defined wave of apoptosis in the intestinal mucosa, starting within several hours after administration of the chemotherapeutic agent. The amplitude of the apoptotic response obtained by either treatments was quite high, being 10 to 20-fold higher than baseline. Respective of the single administration of the chemotherapeutic agent, the resultant apoptotic response was also well defined and subsided after a period of time. Interestingly, there were differences between the two examined chemotherapeutic regimens in the time course of the related induction of apoptosis.

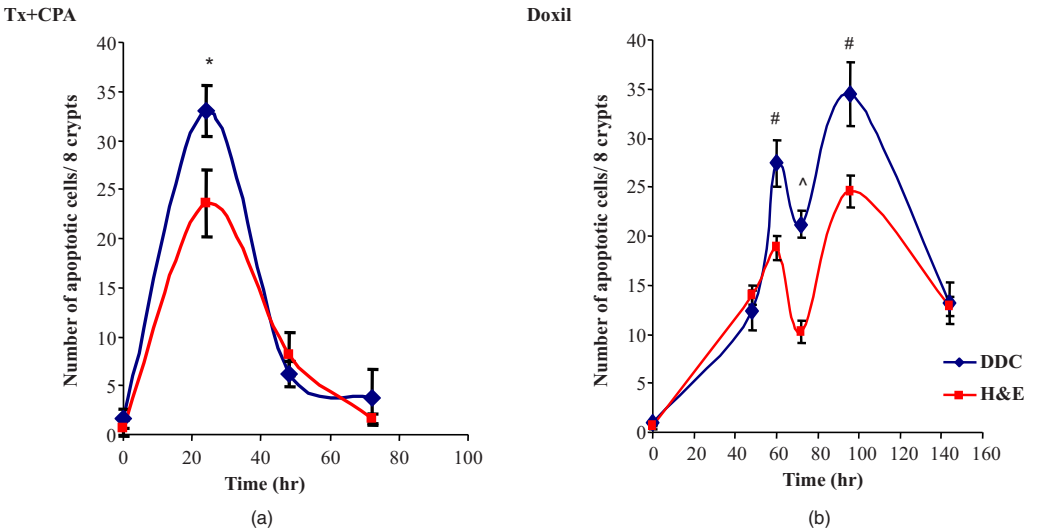

Fig. 3 Temporal profile of chemotherapy-induced DDC uptake by murine ileal epithelium and its correlation with detection of apoptosis by H&E. Assessment of apoptosis in the intestinal mucosa was performed by counting the number of cells manifesting either DDC uptake or apoptotic morphology on H&E staining in 40 consecutive intestinal crypts. The respective analysis was performed on consecutive slides by independent observers, at various time points during 0–144 h after administration of a single dose of either (a) Tx+CPA or (b) doxil #$p<0.05$; *$p<0.005$; ^$p<0.001$.

The wave of apoptosis was monophasic following treatment with taxol+cyclophosphamide, reaching a peak at ~24 h, and subsiding thereafter. In comparison, the peak induced by doxil was biphasic and more prolonged, with peaks at 60 and 100 h, and subsiding by 140 h.

Both intravenous DDC and histological H&E assessment provided strikingly similar reports on the temporal profile and extent of apoptosis induced in the intestinal mucosa by each of the chemotherapeutic regimens (Fig. 3). Moreover, consistently more cells were detected by DDC, as compared to the assessment of apoptosis by H&E. This difference reached a statistical significance at 24 h following the taxol +cyclophosphamide treatment ($p<0.005$), and for the time points of 60, 72, and 96 h after the treatment with doxil ($p<0.05$, $p<0.001$, $p<0.005$, respectively). This observation is conceivable because DDC detects cells from the early stages of the death process, before progression of the death program into gross morphological changes, detectable by H&E. The kinetics of DDC uptake in the tumor is presented in Fig. 4, showing both a quantitative analysis of the DDC-positive cells in the tumor over time [Fig. 4(a)], and demonstrative fluorescent microscopy slides, exemplifying the observation [Fig. 4(b)]. Furthermore, TUNEL staining *ex vivo* supports the kinetic results obtained qualitatively and semi-quantitatively by DDC labeling *in vivo*. Comparison of the temporal profile observed in the ileum to that of the tumor (Fig. 3 versus 4), revealed generally a similar pattern, comprising two apoptotic peaks, with a relatively protracted course spanning 140–160 h after drug administration. Interestingly, the apoptotic wave in the ileum reached its maximal amplitude at the second peak [i.e., at 96 h (Fig. 3)], while maximal apoptotic response in the tumor was observed at the first peak [i.e., at 60 h (Fig. 4)]. This may reflect, as expected, differences between the tumor and ileal cells in the sensitivity and kinetics of the response to the cytotoxic agent.

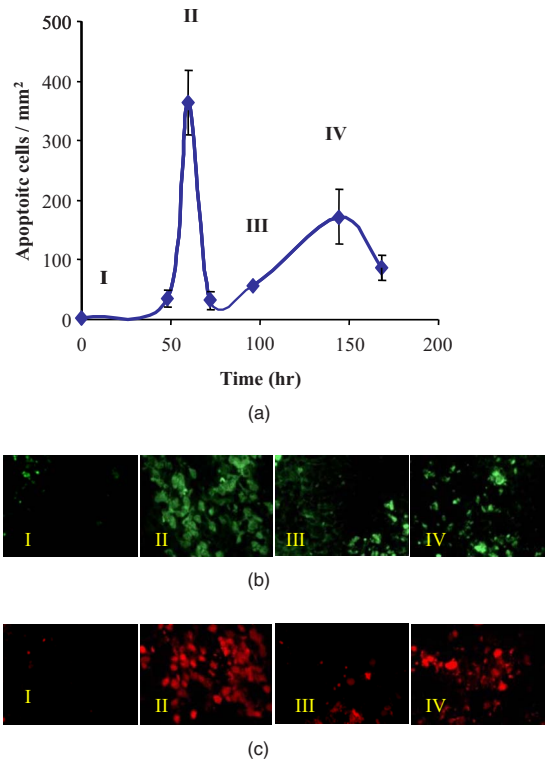

Fig. 4 Assessment of the apoptotic load in C26 tumors. Detection of apoptosis induced in CT26 murine colon carcinoma by systemic administration of a single dose of doxil. (a) Time course of the apoptotic wave detected by DDC. (b) Representative slides at the indicated time points, and (c) Corresponding detection of apoptotic DNA fragmentation by TUNEL.

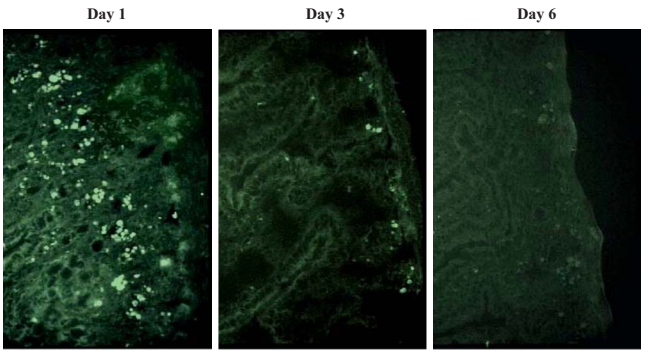

Fig. 5 Fluorescent microscopy of the temporal profile of chemotherapy-induced DDC uptake by murine ileal epithelial cells. DDC-positive cells within the intestinal epithelium, at one, three, and six days after administration of a single dose of Tx+CPA.

The kinetics of the apoptotic response in the ileum following the single dose of a cytotoxic agent is also exemplified in the slides presented in Fig. 5. As shown, numerous DDC-positive cells were detectable in the intestinal mucosa at one day after administration of a single dose of taxol +cyclophosphamide. Far less DDC-positive cells were detectable on day 3 after chemotherapy, while only few cells were detected on day 6. These relatively low-magnification ($\times 200$) fluorescent slides also exemplify the high S/B ratio, created by DDC on its intravenous administration, due to the strong intracellular fluorescence of the apoptotic cells detected by the probe.

4 Discussion

The study presents the performance of the apoptosis biomarker DDC, on its intravenous administration *in vivo*, in detection of apoptosis induced by chemotherapy in the small intestine epithelium. In a murine model, numerous cells with marked DDC uptake were found in the ileal tissue within several hours after administration of anticancer agents. DDC-positive cells were localized in the intestinal crypts (crypts of Lieberkühn), thus matching the sites of dividing stem cells and epithelial regeneration.[19,20] Such dividing cells are known to be prone to the cytotoxic effects of chemotherapy, culminating in induction of apoptosis. Evidently, DDC was capable on its systemic administration *in vivo*, to selectively target these sites. A marked correlation was found between DDC uptake and histological assessment of apoptosis by other methods *ex vivo*, (i.e., TUNEL for DNA cleavage, morphological assessment by H&E, and binding of Annexin-V). Such correlation has also been previously observed in the assessment of DDC in other experimental systems of apoptosis,[10–15] thus further substantiating the performance of this probe as an apoptosis detector. It is noteworthy, however, that it is possible, in addition to apoptosis, chemotherapy triggered also other forms of cell death, such as necrosis or mitotic catastrophe, because positive TUNEL staining has been found in such cells. In addition, there is evidence for transitional forms, taking place *in vivo*, between various programs of cell death. Importantly, similar induction of DDC uptake in ileal tissue was observed for the different cytotoxic regimens examined in the present study, albeit their diverse mechanisms of action (i.e., alkylation, microtubuli disassembly, or topoisomerase II inhibition, for cyclophosphamide, taxol, or doxil, respectively). This finding shows that the performance of DDC is not limited to a specific type of apoptotic trigger, but rather reflects a general feature of detection of apoptotic cells at their occurrence. This observation is also supported by previous reports on DDC.[10,12–15]

The kinetic data of the apoptotic wave detected by DDC and its correlatives (i.e., the TUNEL and H&E assessments) provided several interesting observations. Intestinal epithelium is characterized by a high turnover rate, with mitoses taking place at the crypts of Lieberkühn, followed by gradual migration of the generated cells to the tip of the intestinal villi. Subsequently, these epithelial cells are physiologically eliminated by apoptosis, with rapid clearance and washout of the apoptotic bodies from the tip of the villi by the intestinal fluids. Because of this rapid clearance, few apoptotic cells are normally detectable in ileal tissue at a given time point. By contrast, in chemotherapy-induced enteropathy, the burden of cell death is predominantly at the sites of cell proliferation (i.e., at the crypts of Lieberkühn), thus underlying the often severe, life-threatening clinical implications of this adverse effect of treatment. Indeed, this was also the location of the DDC-positive cells induced by the acute dose of chemotherapy in our study. Importantly, DDC uptake clearly reflected these differences between the physiological and the toxic forms of apoptosis in the ileal tissue, and detected the toxic cryptal damage. Interestingly, as demonstrated in Fig. 5, a shift in the location of the DDC-positive cells toward the tips of the villi was observed between days 1 and 3 after chemotherapy, conceivably reflecting the characteristic cell migration in the ileal epithelium.

Another feature was the ability of DDC to detect differences in the kinetic profiles of the apoptotic waves induced by the different chemotherapeutic regimens. A bipahsic and more protracted time course were found by DDC for doxil treatment, as compared to the taxol+cyclophosphamide regimen (Fig. 3). This profile is anticipated, considering the pharmacokinetic profile of doxil, as previously reported in the literature,[21–23] and conceivably relate, at least in part, to its slow-release properties as a liposomal formulation of doxorubicin. Moreover, this profile of doxil, as found in the ileum was also in alignment with the effect of this drug on the tumor (Fig. 4). In both tissues, a biphasic and protracted apoptotic effect was observed, albeit an interesting difference in the timing of the major apoptotic peak. Taken together, all these data demonstrate the responsiveness of the DDC-signal to the induction, amplitude, and temporal profile of the death process taking place in the examined tissues.

Importantly, at the time points in which DDC detected drug-induced intestinal damage, the examined mice did not manifest any signs of gastrointestinal toxicity, such as weight loss or diarrhea. Enteropathy is a well-known complication observed in patients treated with chemotherapeutic regimens such as those utilized in the present study,[24,25] and, respectively, was also detected by the H&E staining in the treated mice [Fig 1(d)]. Although the mouse model is known to have limitations in assessment of such symptomatology, the findings of the study may support the notion that DDC may provide an *early detection* of intestinal damage, as desired, be-

fore its conversion into overt symptoms and signs.

Several avenues of development may now be pursued, following the current proof-of-concept studies, in order to translate the detection of CIE by DDC into a useful tool for clinical practice. Of specific interest, in our view, is utilization of this probe for a novel optical imaging method. Such a method would take advantage of the inherent fluorescence of DDC and also the superficial location of the intestinal mucosa damaged by the chemotherapy, adjacent to the intestinal lumen. We may therefore envision a method that comprises intravenous administration of DDC, resultant selective accumulation of the probe in the apoptotic cells induced by chemotherapy in the intestinal epithelium, and subsequent visualization of the DDC-positive apoptotic cells by fluorescence endoscopy or endomicroscopy. Indeed, various techniques in the rapidly growing field of endoscopy may be attractive candidates for integration with the DDC test. Among others, these may include confocal endomicroscopy[26–29] or capsule endoscopy.[30,31] Capsule endoscopy, adjusted to fluorescence imaging, looks specifically appealing, due to its noninvasive nature and major usefulness in imaging the small intestine—the major site of CIE. The highly bright spots of the DDC-positive apoptotic cells, as observed in the present study following the intravenous administration of the probe, with high signal/ratio, as exemplified in Fig. 5, seem to strongly support further development in this direction. The next step to be performed in this development would be to advance from visualization by *ex vivo* fluorescence microscopy, as done in the present study, to visualization by endoscopic methods *in vivo*. The paradigm of fluorescence microscopy was found useful for the current proof-of-concept studies and is also frequently used in the development of other molecular imaging probes [i.e., Pittsburg compound –B (PIB) for imaging of amyloid in Alzheimer's disease[32]]. The future development program will focus on construction of an interface associating the fluorescent signal generated by DDC in the apoptotic intestinal cells with the endoscopic method for its capture and visualization. This development will also include optimization of the fluorophore attached to the probe (i.e., red-shift of its excitation wavelength) in order to optimize light penetration depth, reduce potential interference from normal tissue autofluorescence, and avoid excitation with light at the ultraviolet range. Another goal would be the calibration/scaling of the DDC signal obtained from the intestinal epithelium, vis-à-vis the severity of enteropathy, and determination of respective cutoff values of the test.

An alternative approach would be the development of DDC as a probe for positron emission tomography (PET), by attachment of a radioisotope to the molecule (e.g., ^{11}C or ^{18}F). Interestingly, such imaging would be able to provide simultaneous, noninvasive determination of the effect of the cytotoxic agent, both at its target site (i.e., the tumor) where induction of cell death is indeed the desired effect, and at the intestinal mucosa, a site where cell death is the adverse effect of therapy. Indeed, the present study exemplifies this approach, by showing the utility of intravenous DDC *in vivo*, in reporting on the effect of doxil at both the tumor and the ileum. Accordingly, such imaging of apoptosis may be an attractive approach for early, noninvasive molecular characterization of the *efficacy/toxicity balance* of anticancer regimens, a critical factor in clinical decision-making in oncology.

Either fluorescence imaging with DDC, or PET imaging with a radio-labeled derivative of the probe, may therefore introduce molecular imaging into the assessment of CIE. Considering the high prevalence of chemotherapy-induced enteropathy and the difficulty in its prediction, such molecular imaging may be valuable for clinical practice. By providing molecular imaging of the tissue damage *in situ*, at the cellular level, before its translation into overt clinical symptoms and signs, DDC may advance careful monitoring of this prevalent adverse effect of cytotoxic agents and assist in early adjustment of therapy, when required, in order to optimize treatment for the individual cancer patient.

Acknowledgment

DDC is an investigational imaging agent developed by Aposense Ltd. (formerly NST Ltd.).

References

1. D. M. Keefe, J. Brealey, G. J. Goland, and A. G. Cummins, "Chemotherapy for cancer causes apoptosis that precedes hypoplasia in crypts of the small intestine in humans," *Gut* **47**(5), 632–637 (2000).
2. J. A. Daniels, M. K. Gibson, L. Xu, S. Sun, M. I. Canto, E. Heath, J. Wang, M. Brock, and E. Montgomery, "Gastrointestinal tract epithelial changes associated with taxanes: marker of drug toxicity versus effect," *Am. J. Surg. Pathol.* **32**(3), 473–477 (2008).
3. K. A. Bell, A. G. Perna, and S. Hsu, "Mucositis as a treatment-limiting side effect in the use of capecitabine for the treatment of metastatic breast cancer," *J. Am. Acad. Dermatol.* **45**(5), 790–791 (2001).
4. P. G. Rose and M. S. Piver, "Intestinal perforation secondary to paclitaxel," *Gynecol. Oncol.* **57**(2), 270–272 (1995).
5. C. A. Iacobuzio-Donahue, E. L. Lee, S. C. Abraham, J. H. Yardley, and T. T. Wu, "Colchicine toxicity: distinct morphologic findings in gastrointestinal biopsies," *Am. J. Surg. Pathol.* **25**(8), 1067–1073 (2001).
6. C. Eng, "Toxic effects and their management: daily clinical challenges in the treatment of colorectal cancer," *Nat. Rev. Clin. Oncol.* **6**(4), 207–218 (2009).
7. J. M. Bowen, R. J. Gibson, A. Tsykin, A. M. Stringer, R. M. Logan, and D. M. Keefe, "Gene expression analysis of multiple gastrointestinal regions reveals activation of common cell regulatory pathways following cytotoxic chemotherapy," *Int. J. Cancer* **121**(8), 1847–1856 (2007).
8. D. Sandmeier, P. Chaubert, and H. Bouzourene, "Irinotecan-induced colitis," *Int. J. Surg. Pathol.* **13**(2), 215–218 (2005).
9. R. J. Gibson and D. M. Keefe, "Cancer chemotherapy-induced diarrhoea and constipation: mechanisms of damage and prevention strategies," *Support Care Cancer* **14**(9), 890–900 (2006).
10. A. Reshef, A. Shirvan, E. Shohami, H. Grimberg, G. Levin, A. Cohen, V. Trembovler, and I. Ziv, "Targeting cell death *in vivo* in experimental traumatic brain injury by a novel molecular probe," *J. Neurotrauma* **25**(6), 569–580 (2008).
11. A. Cohen, I. Ziv, T. Aloya, G. Levin, D. Kidron, H. Grimberg, A. Reshef, and A. Shirvan, "Monitoring of chemotherapy-induced cell death in melanoma tumors by N,N′-Didansyl-L-cystine," *Technol. Cancer Res. Treat.* **6**(3), 221–234 (2007).
12. R. Aloya, A. Shirvan, H. Grimberg, A. Reshef, G. Levin, D. Kidron, A. Cohen, and I. Ziv, "Molecular imaging of cell death *in vivo* by a novel small molecule probe," *Apoptosis* **11**(12), 2089–2101 (2006).
13. M. Damianovich, I. Ziv, S. N. Heyman, S. Rosen, A. Shina, D. Kidron, T. Aloya, H. Grimberg, G. Levin, A. Reshef, A. Bentolila, A. Cohen, and A. Shirvan, "ApoSense: a novel technology for functional molecular imaging of cell death in models of acute renal tubular necrosis," *Eur. J. Nucl. Med. Mol. Imaging* **33**(3), 281–291 (2006).
14. A. Reshef, A. Shirvan, H. Grimberg, G. Levin, A. Cohen, A. Mayk, D. Kidron, R. Djaldetti, E. Melamed, and I. Ziv, "Novel molecular imaging of cell death in experimental cerebral stroke," *Brain Res.* **1144**, 156–164 (2007).

15. A. Reshef, A. Shirvan, R. N. Waterhouse, H. Grimberg, G. Levin, A. Cohen, L. G. Ulysse, G. Friedman, G. Antoni, and I. Ziv, "Molecular imaging of neurovascular cell death in experimental cerebral stroke by PET," *J. Nucl. Med.* **49**(9), 1520–1528 (2008).
16. Y. Gavrieli, Y. Sherman, and S. A. Ben-Sasson, "Identification of programmed cell death in situ via specific labeling of nuclear, DNA fragmentation," *J. Cell Biol.* **119**(3), 493–501 (1992).
17. J. H. Garcia, Y. Yoshida, H. Chen, Y. Li, Z. G. Zhang, J. Lian, S. Chen, and M. Chopp, "Progression from ischemic injury to infarct following middle cerebral artery occlusion in the rat," *Am. J. Pathol.* **142**(2), 623–35 (1993).
18. C. B. Drachenberg, O. B. Ioffe, and J. C. Papadimitriou, "Progressive increase of apoptosis in prostatic intraepithelial neoplasia and carcinoma: comparison between in situ end-labeling of fragmented DNA and detection by routine hematoxylin-eosin staining," *Arch. Pathol. Lab Med.* **121**(1), 54–58 (1997).
19. N. Barker, M. van de Wetering, and H. Clevers, "The intestinal stem cell," *Genes Dev.* **22**(14), 1856–1864 (2008).
20. T. H. Yen and N. A. Wright, "The gastrointestinal tract stem cell niche," *Stem Cell Rev.* **2**(3), 203–212 (2006).
21. K. M. Laginha, S. Verwoert, G. J. Charrois, and T. M. Allen, "Determination of doxorubicin levels in whole tumor and tumor nuclei in murine breast cancer tumors," *Clin. Cancer Res.* **11**(19 Pt 1), 6944–6949 (2005).
22. G. J. Charrois and T. M. Allen, "Multiple injections of pegylated liposomal Doxorubicin: pharmacokinetics and therapeutic activity," *J. Pharmacol. Exp. Ther.* **306**(3), 1058–1067 (2003).
23. T. A. Elbayoumi and V. P. Torchilin, "Tumor-specific antibody-mediated targeted delivery of Doxil reduces the manifestation of auricular erythema side effect in mice," *Int. J. Pharm.* **357**, 272–279 (2008).
24. V. L. Seewaldt, J. M. Cain, B. A. Goff, H. Tamini, B. Greer, and D. Figge, "A retrospective review of paclitaxel-associated gastrointestinal necrosis in patients with epithelial ovarian cancer," *Gynecol. Oncol.* **67**, 137–140 (1997).
25. N. S. Thakkar and C. S. Potten, "Abrogation of adriamycin toxicity *in vivo* by cycloheximide," *Biochem. Pharmacol.* **43**(8), 1683–1691 (1992).
26. K. Venkatesh, M. Cohen, C. Evans, P. Delaney, S. Thomas, C. Taylor, A. Abou-Taleb, R. Kiesslich, and M. Thomson, "Feasibility of confocal endomicroscopy in the diagnosis of pediatric gastrointestinal disorders," *World J. Gastroenterol.* **15**(18), 2214–2219 (2009).
27. R. S. Dacosta, B. C. Wilson, and N. E. Marcon, "New optical technologies for earlier endoscopic diagnosis of premalignant gastrointestinal lesions," *J. Gastroenterol. Hepatol* **17**(Suppl), S85–104 (2002).
28. H. Inoue, S. E. Kudo, and A. Shiokawa, "Technology insight: laser-scanning confocal microscopy and endocytoscopy for cellular observation of the gastrointestinal tract," *Nat. Clin. Pract. Gastroenterol. Hepatol.* **2**(1), 31–37 (2005).
29. P. L. Hsiung, J. Hardy, S. Friedland, R. Soetikno, C. B. Du, A. P. Wu, P. Sahbaie, J. M. Crawford, A. W. Lowe, C. H. Contag, and T. D. Wang, "Detection of colonic dysplasia *in vivo* using a targeted heptapeptide and confocal microendoscopy," *Ther. Immunol.* **14**(4), 454–458 (2008).
30. A. Moglia, A. Menciassi, P. Dario, and A. Cuschieri, "Capsule endoscopy: progress update and challenges ahead," *Nat. Rev. Gastroenterol. Hepatol.* **6**(6), 353–362 (2009).
31. H. Zhang, D. Morgan, G. Cecil, A. Burkholder, N. Ramocki, B. Scull, and P. K. Lund, "Biochromoendoscopy: molecular imaging with capsule endoscopy for detection of adenomas of the, GI tract," *Gastrointest. Endosc.* **68**(3), 520–527 (2008).
32. B. J. Bacskai, G. A. Hickey, J. Skoch, S. T. Kajdasz, Y. Wang, G. F. Huang, C. A. Mathis, W. E. Klunk, and B. T. Hyman, "Four-dimensional multiphoton imaging of brain entry, amyloid binding, and clearance of an amyloid-beta ligand in transgenic mice," *Proc. Natl. Acad. Sci. U.S.A.* **100**(21), 12462–12467 (2003).